Cooperative Spin-State Switching and Vapochromism of Mononuclear Ni(II) Complexes by Pyridine Coordination/Decoordination

Sotaro Kusumoto, Kazumasa Inaba, Harutoshi Suda, Manabu Nakaya, Ryuya Tokunaga, Pierre Thuéry, Rie Haruki, Tomoki Kanazawa, Shunsuke Nozawa, Yang Kim, et al.

Cooperative spin-state switching and vapochromism of mononuclear Ni(II) complexes by pyridine coordination/de-coordination

Sotaro Kusumoto,*[a] Kazumasa Inaba,[a] Harutoshi Suda,[a] Manabu Nakaya,[b] Ryuya Tokunaga,[c] Pierre Thuéry,[d] Rie Haruki,[e] Tomoki Kanazawa,[e] Shunsuke Nozawa,[e] Yang Kim,[c] Shinya Hayami,[c,f] Yoshihiro Koide*[a]

[a] *Department of Material and Life Chemistry, Faculty of Engineering, Kanagawa University, 3-27-1 Rokkakubashi, Kanagawa-ku, Yokohama 221-8686, Japan. E-mail: kusumoto@kanagawa-u.ac.jp.*
[b] *Department of Chemistry, Faculty of Science, Josai University, 1-1 Keyakidai, Sakado, Saitama 350-0295, Japan.*
[c] *Department of Chemistry, Graduate School of Science and Technology, Kumamoto University, 2-39-1 Kurokami, Chuo-ku, Kumamoto 860-8555, Japan.*
[d] *Université Paris-Saclay, CEA, CNRS, NIMBE, 91191 Gif-sur-Yvette, France.*
[e] *Photon Factory, Institute of Materials Structure Science, High Energy Accelerator Research Organization (KEK), 1-1 Oho, Tsukuba, Ibaraki 305-0801, Japan*
[f] *Institute of Industrial Nanomaterials (IINa), Kumamoto University, 2-39-1 Kurokami, Chuo-ku, Kumamoto 860-8555, Japan.*
KEYWORDS; Pyridine • Nickel Complexes • Vapochromism • CISSS • Spin-State Switching

ABSTRACT

Two mononuclear Ni(II) complexes (**1** and **2**) have been found to display color changes upon coordination/decoordination of pyridine, resulting in their structural transformation between square-planar and octahedral geometries as well as a change in their spin state. Compound **1** changes between red (**1r**) and yellow (**1y**) upon exposure to or elimination of pyridine, while **2** undergoes a two-step transformation, changing orange **2o** (S = 0) ⇄ gray **2g'** (S = 1) → yellow **2y'** (S = 1) depending on the reaction time. The first step (**2o**→**2g'**) takes less than 45 minutes, which is significantly faster than the previously reported reaction time of one day for a Ni(II) complex/pyridine vapor system. The **2o** reacting with pyridine can be easily prepared by dispersing **2g** in methanol instead of annealing at high temperatures (130 °C), which can be applied to develop chemical sensors for pyridine utilizing color changes and/or magnetic switching.

INTRODUCTION

The development of solid-state systems with magnetic properties dependent on reactions with volatile organic compounds (VOCs) is attracting a lot of attention due to their potential applications as chemical sensors.[1] Spin crossover (SCO) complexes that change due to the interaction between organic solvents or gas molecules and the central metal ion in the complex have been well-studied as magnetic sensors,[2] among which Fe(II)-MOFs (metal-organic frameworks) are attractive because they can be detected both magnetically and visually by causing spin transition between high spin (HS) (S = 2) and low spin (LS) (S = 0).[3] Guest molecules are typically trapped within crystals by weak supramolecular interactions, which are usually unstable and limit the range of operating temperatures as sensors. Therefore, materials capable of changing magnetic properties through coordination bond formation between host-guest molecules, known as 'coordination induced spin-state switching' (CISSS),[4] have been expected to be high stability and selectivity and to be better chemical sensors operating at room temperature with respect to organic compounds. This can be applied to the measurement of volatile coordination solvents such as alcohol, pyridine, ammonia, amine, etc.[5] Materials that exhibit both CISSS and color changes are promising not only as magnetic sensors but also as color-identifiable chemical sensors, even though they have been mainly studied in solution, with few reports of solid state systems.[4,5] As a promising approach to the development of these systems, Ni(II) complexes can be used because color changes of the compounds are observed, associated with diamagnetism (S = 0) in four-coordinate square-planar geometry and paramagnetism (S = 1) in a five-coordinate square-pyramidal or six-coordinate octahedral geometry.[5] In the solid state, the CISSS between S = 0 and S = 1 gives a methanol-selective vapochromic response in a mononuclear Ni(II)-quinonoid (quinonoid = 4-methylamino-6-methyliminio-3-oxocyclohexa-1,4-dien-1-olate) complex.[5a] More

recently, the vapochromism and magnetochemical switching by reversible NH_3 uptake and release in dinuclear $[Ni_2(Pn)_4]$ (PnH = 6-*tert*-butyl-pyridazine-3-thione),[5b] and the spin state switching between octahedral paramagnetic and square-planar diamagnetic behavior depending on the absorption/desorption of axially coordinated pyridine in $[Ni_2(hbth)(py)_6]\cdot 2MeOH$ (H_4hbth = *N*′1,*N*′4-bis((*E*)-2-hydroxybenzylidene)terephthalohydrazide)[5c] have been demonstrated. Despite the pioneering nature of these studies, the development of faster systems is crucial for advancing sensing materials, as the protracted transformation times in these systems hinder their efficiency and optimization.

In this study, Ni(II) complexes capable of vapochromism and CISSS with square-planar geometry in which chelating ligands **L**[1] (HL^1 = 2-hydroxy-*N*'-((1*E*,2*E*)-3-phenylallylidene)benzohydrazide) and **L**[2] (HL^2 = (*E*)-2-hydroxy-*N*'-(4-methylbenzylidene)benzohydrazide) are separately coordinated will be investigated for color and magnetic transformation by coordination/decoordination of volatile organic molecules, thereby demonstrating the possibility as fast-acting sensors (Scheme 1).

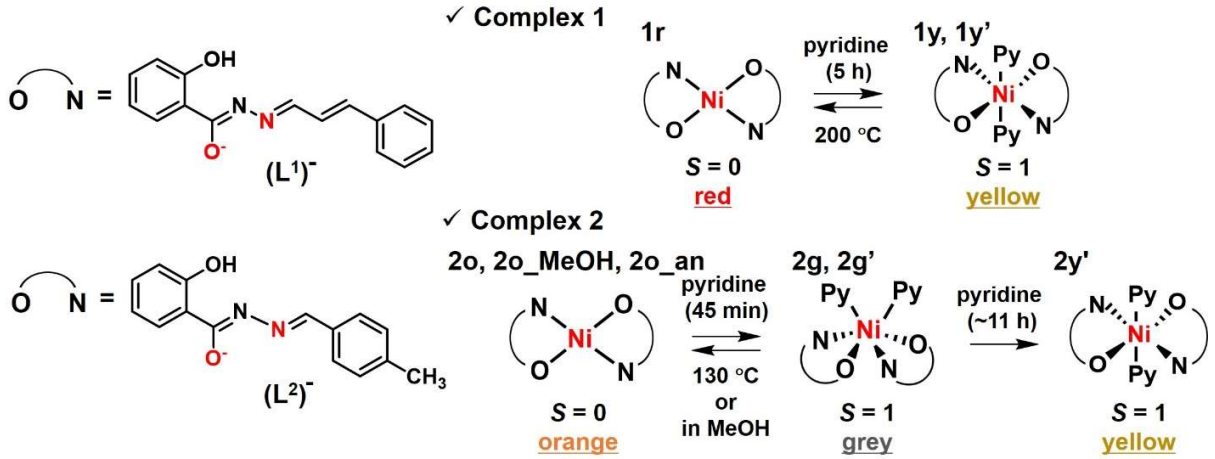

Scheme 1. Color change and spin-state switching of Ni(II) complexes **1** and **2** in the solid state.

RESULTS AND DISCUSSION

Vapochromism

Ligand H**L**[1] was obtained by reacting salicylamide with *trans*-cinnamaldehyde (Scheme S1), and was then reacted with $NiCl_2 \cdot 6H_2O$ and pyridine to produce **1y**, a yellow powder (Figure 1 and Scheme S2).[6] The yellow complex (**1y**) changed to red (**1r**) when heated on a 200 °C hot plate and returned to yellow when exposed to pyridine vapor (Figure 1a). This result can be explained by a phenomenon caused by the coordination/decoordination of pyridine molecules, which is supported by the result of mass loss corresponding to two pyridine molecules near 200 °C from thermal gravimetric analysis (TGA) (Figure 2a). When the red compound (**1r**) is re-exposed to pyridine vapor, it is changed to yellow powder (**1y′**) (Figure 1a), thereby enabling vapochromism by pyridine. However, although the TGA of **1y′** results in a mass loss of two equivalents of pyridine molecules, the decoordinating temperature of pyridine was about 130 °C (Figure S1), unlike **1y**, confirming that **1y′** has a packing structure different from that of **1y,** as shown by powder X-ray diffraction (PXRD) (Figure S2). Ni(II) salt and pyridine were reacted with H**L**[2] prepared using salicylamide and *p*-tolualdehyde to give a grey Ni(II) complex (**2g**) (Figure 1b and Scheme S2), which was changed to orange by annealing on a hot plate at 130 °C (**2o_an**) (Figure 1b) and showed the mass loss of two pyridine molecules near 130 °C as well by TGA (Figure 2b). The orange **2o_an** was returned to grey (**2g'**) within an hour by exposure to pyridine vapor, with the same PXRD as the original **2g** (Figure 2c). After an additional 12 hours of exposure to pyridine, **2g'** changed to yellow (**2y'**) (Figure 1b), and elemental analysis of the latter showed that it contained four pyridine molecules. Although we have not succeeded in obtaining a crystal structure of **2y'**, it seems to contain two pyridine molecules in each of the first and second coordination spheres. As a result of attempting to anneal yellow **2y'** in the same way as **2g**, it turned

orange directly without going through a grey **2g'** compound by heating. Interestingly, the same color change scheme (orange ⇌ grey → yellow) through coordination/decoordination was observed when this process was repeated (Figure 2d), showing the potential of **2** as a recyclable chemical sensor for pyridine based on vapochromism. To obtain orange **2o_MeOH** in which two pyridine molecules were de-coordinated by methanol, the grey **2g** was dispersed in methanol and ultrasonicated for 20 seconds (Figure 1b and Video 1). According to PXRD, **2o_an** lost its crystallinity while **2o_MeOH** retained it, with a pattern well consistent with that simulated from the crystal structure of **2o** (Figure 2c). However, this method could not be applied to **1** due to its good solubility in methanol. By exposing **2o_MeOH** to the vapor of several volatile organic solvents, their selectivity was investigated using PXRD, but only pyridine was selectively reacted, and most common solvents were not (Figure S3). The time-dependent reaction by pyridine vapor exposure (Figure S4) for both **1r** and **2o_an** was estimated using PXRD (Figures 2e and 2f). The former changed to **1y'** after 5 hours, recovering crystallinity similar to **1y**, while the latter showed a packing structure (**2g'**) similar to **2g** after 45 minutes and changed to yellow (**2y'**) after 11 hours (Figures 1b and S5). These results show that these complexes undergo vaporochromism by pyridine in a relatively short time, probably due to the change in the geometry of the environment of the labile Ni(II) ion, square-planar or octahedral, through coordination/decoordination of pyridine, and that they can be used as chemical sensors of pyridine.

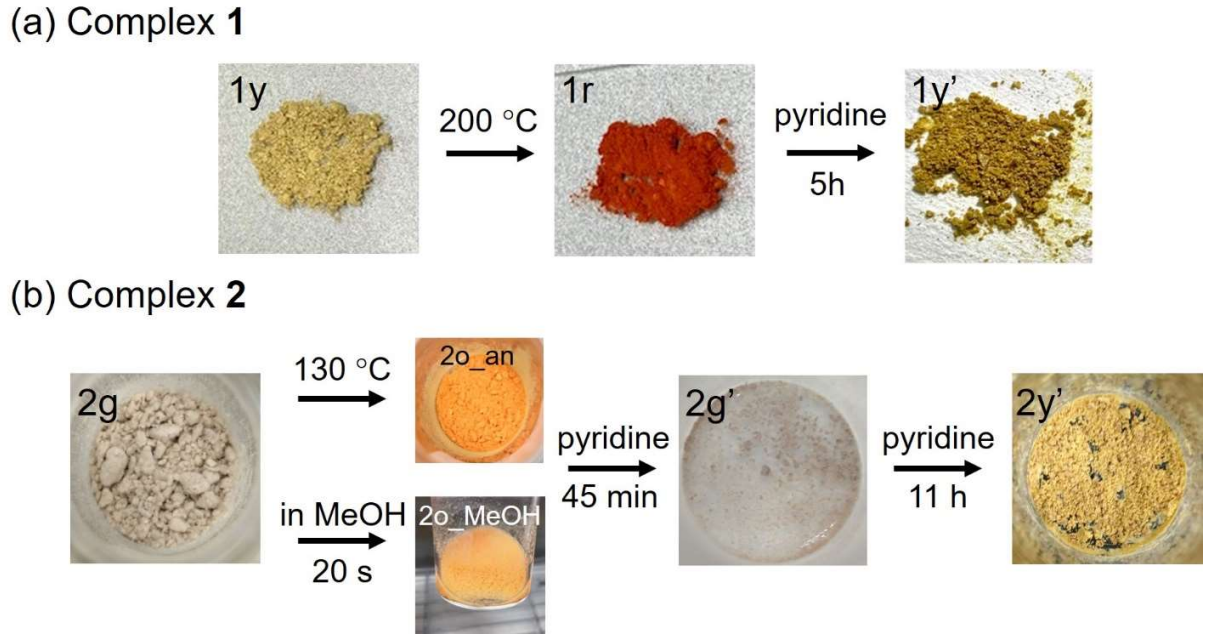

Figure 1. Color change of compounds **1** (a) and **2** (b) by heating and pyridine exposure.

(**2o_MeOH** was prepared by dispersing **2g** in methanol.)

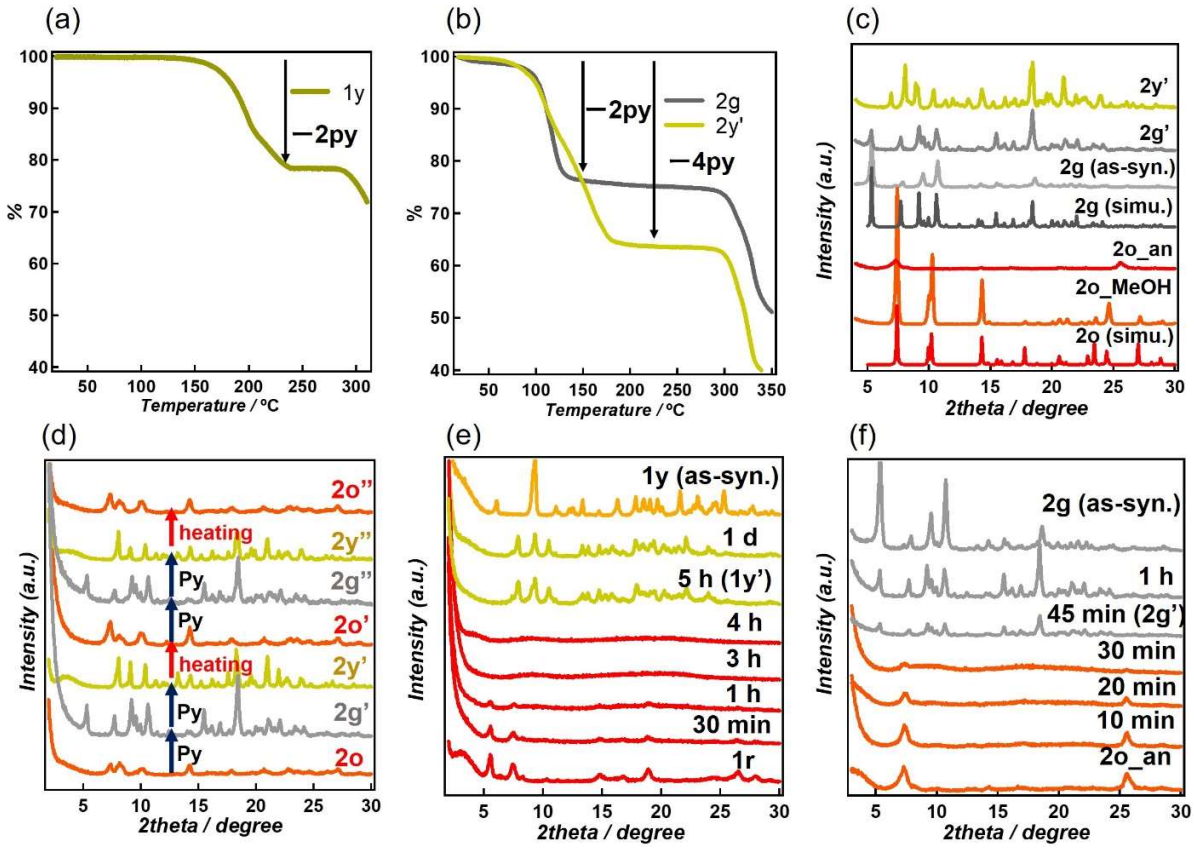

Figure 2. TGA of compounds **1** and **2** (**1y** (a), **2g** (b), and **2y'** (b). Py is pyridine.). Changes in PXRD patterns of several compounds ((c), PXRD related to compound **2**; (d), Repeated exposure and heating of pyridine in compound **2**; (e), Time-dependent pyridine exposure of **1r**; (f), Time-dependent pyridine exposure of **2o_an**; simu. = Simulation; as-syn. = Raw compounds as synthesized).

Structural characterization

Single crystal X-ray diffraction analysis (SCXRD) was carried out to investigate the transformation of the molecular structures of the above compounds by vapochromism. The chloroform solution of an annealed **1y** was slowly evaporated to give red plate-like crystals **1r** as monoclinic with space group $P2_1/n$, in which an imine nitrogen and carbonyl anion in each

deprotonated ligand were coordinated to Ni(II) to produce a square-planar geometry (Figure 3a, Table S1). It is composed of a one-dimensional (1D) slip-stacked structure by π-π stacking interactions with an intermetallic distance of 4.096 Å along the *a*-axis (Figure S6) as well as C-H---π interactions (*d* = 3.384 Å) between two molecules (Figure S7). The crystal structure of **1y** has already been reported,[6] which has been crystallized into triclinic *P*-1 with the structural formula [Ni($\mathbf{L^1}$)$_2$(pyridine)$_2$]. Carbonyl anion and imine nitrogen of each deprotonated chelate ligand are coordinated in the equatorial plane of Ni(II), and its two axial positions are occupied by two pyridine molecules to give an octahedral geometry (Figure 3b). Its packing structure gives a zig-zag 1D chain along the *b*-axis by CH---π interaction (*d* = 2.779 Å) between *para*-hydrogen of axial pyridine and equatorial-benzene ring of neighboring molecules (Figure S8), resulting in a 2D structure by interacting (*d* = 2.597 Å) between hydroxyl group in the salicylhydrazide moiety and *meta*-hydrogen of adjacent pyridine molecule along the *a*-axis (Figure S9). Orange plate-like crystals **2o**, monoclinic with space group *C*2/*c*, were prepared from chloroform solution of **2o_an** to give a four-coordinate square-planar structure with bond lengths of Ni-N (*d* = 1.872 Å) and Ni-O (*d* = 1.838 Å) similar to those of **1r** and other square-planar Ni(II) complexes (Table S2),[5a, 7] showing a slip-stacked structure through Ni---π interactions (*d* = 3.447 Å) along the *b*-axis direction (Figure S10). Single crystals **2g** with space group *P*2$_1$/*c* were prepared from methanolic solution, and unlike **1y** (Figure 3b), their structure displays an octahedral geometry occupied by two bidentate ligands and two *cis*-positioned pyridine molecules (Figure 3d). The Ni-N (*d* = 2.076-2.101 Å) and Ni-O bond distances (*d* = 2.033 and 2.045 Å) are similar to those in **1y** and other octahedral Ni(II) complexes.[8] Each of the discrete molecules interacts with neighboring molecules in various ways, such as CH---π (*d* = 3.659, 3.297, 3.259, 3.215, 2.939, 2.503 Å) and CH---O (*d* = 2.544 Å) (Figure S11).

The shoulders of solid-state electronic absorption spectra observed at ~500 nm for **1r** and **2o** are considered charge transfer from the [NiN_2O_2] to the electron-accepting ligand (Figure S12).[5d] The weak absorption bands around 580 and 800 nm for **1y**, **2g**, and **2y'** are attributed to $^3A_{2g}\rightarrow{}^3T_{2g}$ and $^3A_{2g}\rightarrow{}^3T_{1g}$, which correspond to typical *d-d* transition for octahedral Ni(II).[5d]

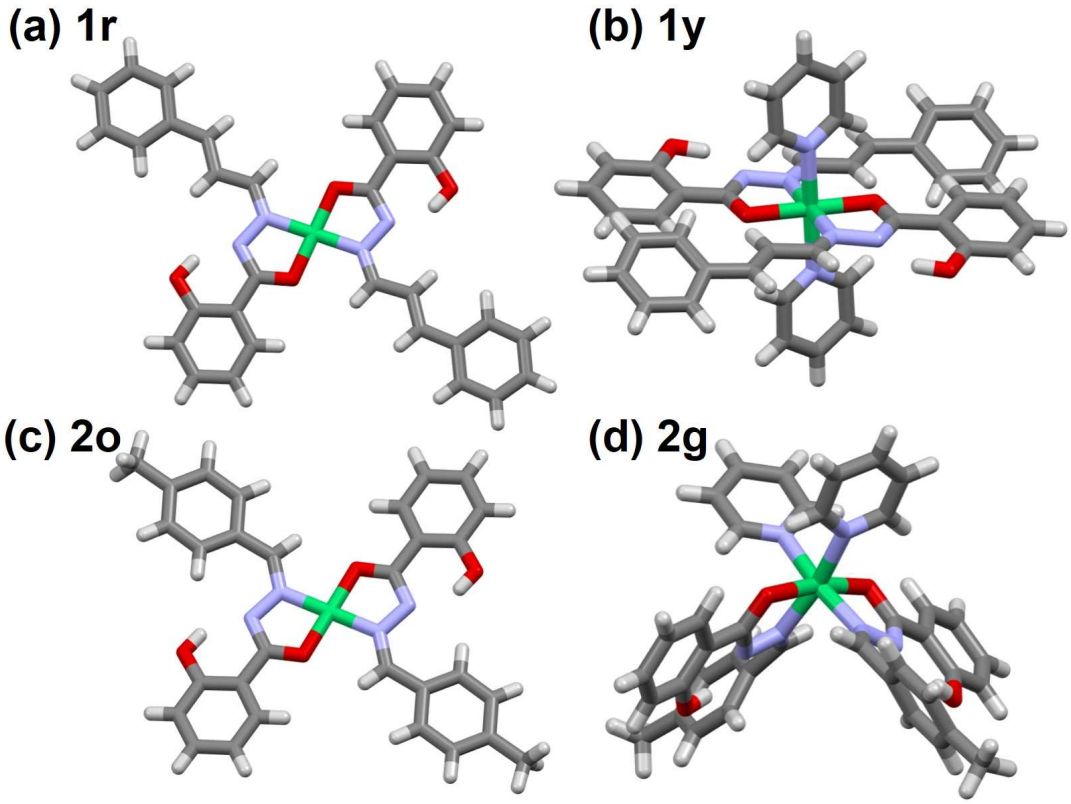

Figure 3. (a) Crystal structures of **1r** (a), **1y** (b), **2o** (c), and **2g** (d).

Correlation between reaction time with pyridine and structural stability from the theoretical calculation

From the PXRD time-dependence upon pyridine exposure discussed above, the time required for transformation of four-coordinate square-planar **1r** into six-coordinate octahedral **1y'** is 5 hours, and only 45 minutes for **2o** to **2g'**. An energy framework analysis was performed to discuss these differences in terms of packing stability (Figures 4 and S13-14).[9] The π-π stacking of complex **1r**

along the *a*-axis results in very high stabilization with a total energy (E_{tot}) of -127.1 kJ/mol, and the second strong energy is -45.9 kJ/mol (Figure S13). On the other hand, E_{tot} of **2o** based on Ni--π interaction is -101.3 kJ/mol, which is 25.8 kJ/mol less stable than **1r**, and the second strong energy is -37.2 kJ/mol, which is 8.7 kJ/mol less stable (Figure S14). This suggests that the **1r** molecule has stronger π-π and CH-π interactions with neighboring molecules than **2o**, making it more difficult to introduce the pyridine molecules required for the extension to six-coordinate geometry, resulting in different speeds.

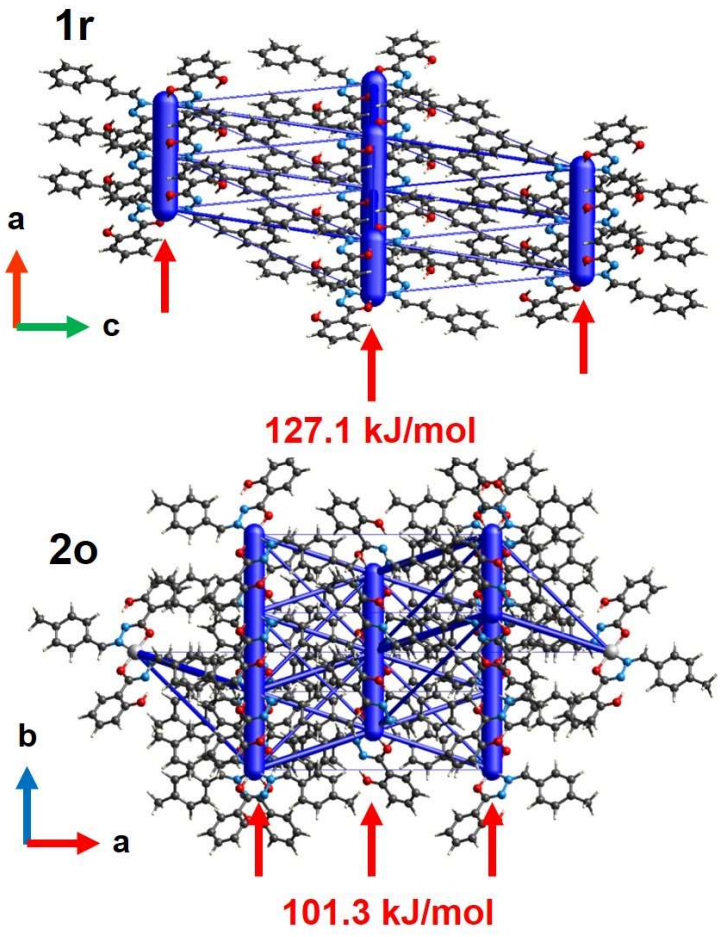

Figure 4. Energy framework calculation in total interaction strengths for **1r** and **2o**. The thickness of the blue tube corresponds to the level of stabilization energy for each dimer.

X-ray absorption fine structure (XAFS) measurements

X-ray absorption fine structure (XAFS) measurements were performed to obtain information on the local structures of **1r**, **1y'**, and **2y'**, for which the PXRDs do not match the crystal structure-based simulations (Figures 2c and S2) or where crystal structures are not present. The k^2-weighted Ni K-edge Extended X-ray Absorption Fine Structure (EXAFS) of **1y**, **1y'**, **2g**, and **2y'** (Figure 5a) show almost the same broad peaks at 1.63 Å, indicating that the bond distances around Ni(II), that is, the [N_4O_2] coordination sphere, are the same. The peaks of **1r** and **2o_an** from which pyridine ligands were removed were observed at 1.42 Å, indicating shorter bond distances than **1y**, **1y'**, **2g**, and **2y'**, and also consistent with forming square-plane structure.[10a] In the X-ray absorption near edge structure (XANES) region, **1y**, **1y'**, **2g**, and **2y'** show the same absorption edges (Figure 5b), which is similar to the octahedral Ni(II) geometry. [10] The shoulders of **1r** and **2o_an** near 8340 eV are due to the destabilization of nearly degenerated $4p_x$ and $4p_y$ orbitals concerning the $4p_z$ orbital in the square-planar Ni(II) complexes, and thus dipole-allowed $1s \rightarrow 4p_z$ absorption is observed as a shoulder peak. The pre-edge peak of **1r** and **2o_an** at 8333 eV are assigned to the $1s \rightarrow 3dx^2\text{-}y^2$ absorption, and $3dx^2\text{-}y^2$ is an unoccupied orbital.[10] For **1r**, the simulated PXRD and that of the annealed complex do not match each other, but the XAFS result suggests a square-planar structure. In the case of **2y'**, the XAFS result suggests an octahedral structure of [N_4O_2] and is expected to form a *trans*-isomer similar to that of **1y** due to the color change to yellow.

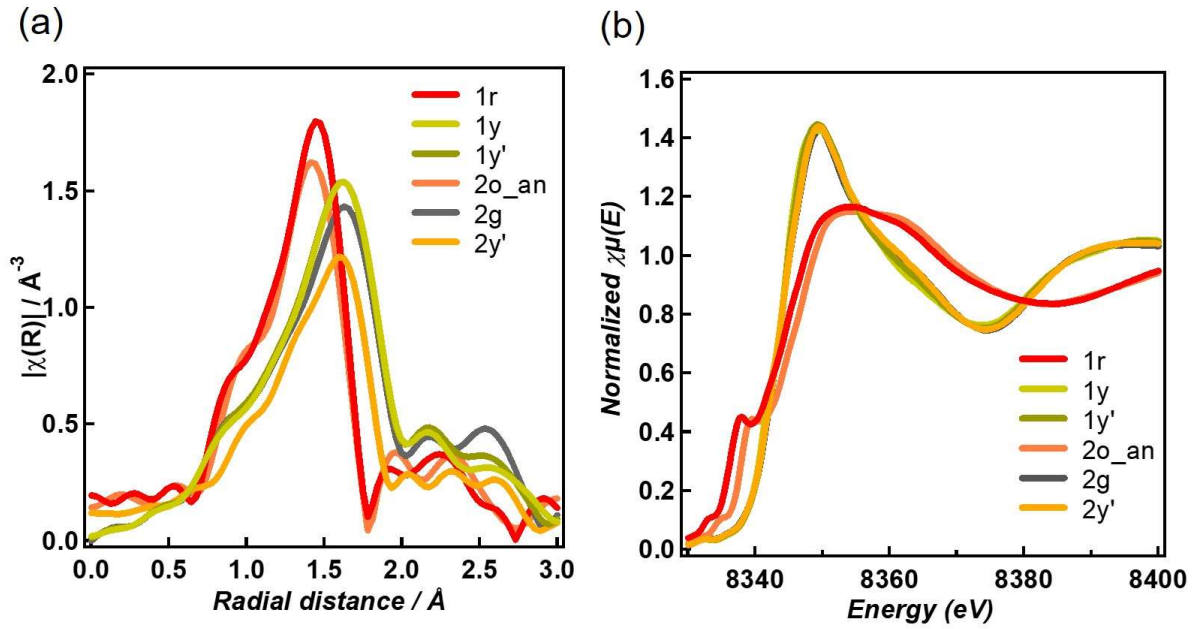

Figure 5. (a) EXAFS Fourier transform (a) and XANES spectra (b) of the Ni-K edge of compounds **1r**, **1y**, **1y'**, **2o_an**, **2g**, and **2y'**.

Magnetic switching by coordination/decoordination of pyridine

SCXRD and XAFS reveal that the vapochromism is derived from the changes in the coordination number and geometry between square-planar (S = 0) and octahedral (S = 1) by coordination/decoordination of pyridine molecules, and thus an associated magnetic transformation is expected. The temperature-dependent magnetic susceptibilities were measured using a Superconducting Quantum Interference Device (SQUID) in the 2–300 K at 5000 Oe (Figures 6 and S15). The χ_mT values of **1r**, **2o_MeOH**, and **2o_an** are almost 0 cm^3 K mol^{-1}, and **1y'**, **2g'**, and **2y'** are 1 cm^3 K mol^{-1}, respectively, which correspond not only to the theoretical values for the diamagnetic (S = 0) and paramagnetic (S = 1) mononuclear Ni(II) complex but also to the results that **1r** and **2o** are square planar and **1y**, **2g'** and **2y'** are octahedral, as shown above by SCXRD and XAFS. On lowering the temperature, the χ_mT shows an abrupt decrease below 10 K in **1y'**, **2g'**, and **2y'**, which is attributable to the intramolecular antiferromagnetic interaction or

a zero-field splitting (ZFS). Magnetic switching between **2o_an** ($S = 0$) and **2g'** ($S = 1$) compounds are repeatedly possible (Figure 6b), and this compound has the potential as a recyclable chemical sensor for pyridine because both spin state and color can change by the coordination/decoordination of pyridine molecules.

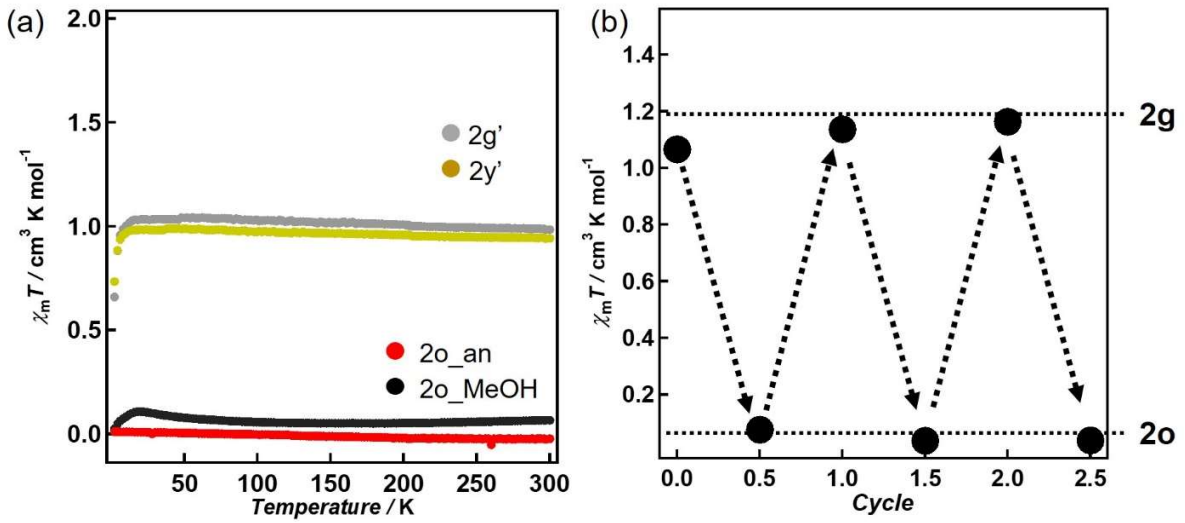

Figure 6. (a) Temperature-dependent magnetic susceptibilities of **2o_an**, **2o_MeOH**, **2g'**, and **2y'**. (b) Magnetic switching between **2o** and **2g** via coordination/decoordination of pyridine molecules.

CONCLUSIONS

Mononuclear, discrete Ni(II) complexes with ligands H**L**^{1} or H**L**^{2} change their geometry through coordination/decoordination of pyridine molecules, resulting in a change in color and magnetic properties, which could be repeated and was investigated by SCXRD and XAFS methods. The vapochromism of Ni(II) complexes by pyridine molecules is completed in two steps, which is reported for the first time among related CISSS systems and enable the development of new molecules capable of switching color and/or magnetism in the solid state. Given the results, the

Ni(II) compounds proposed in this study provide potential applications for chemical sensors and memory devices.

Acknowledgements: S. K. is thankful for the financial support received from KAKENHI Grant-in-Aid for Early-Career Scientists JP22K14698 and the Iketani Science and Technology Foundation. The XAFS measurements were performed with approval by the KEK Photon Factory program 2022P015.

ASSOCIATED CONTENT

Accession Codes

CCDC 2256036−2256038 contain the supplementary crystallographic data for this paper. These data can be obtained free of charge via www.ccdc.cam.ac.uk/data_request/cif, or by emailing data_request@ccdc.cam.ac.uk, or by contacting The Cambridge Crystallographic Data Centre, 12 Union Road, Cambridge CB2 1EZ, UK; fax: +44 1223 336033.

Supporting Information

The Supporting Information is available free of charge at XXXX.

Detailed synthesis of ligands and Ni complexes, crystal parameter and structure data of Ni complexes, PXRD, TGA and diffused reflectance results of Ni complexes, energy framework calculation of **1r** and **2o**, etc. (PDF).

AUTHOR INFORMATION

Corresponding Authors

*E-mail: kusumoto@kanagawa-u.ac.jp (S.K.)

*E-mail: ykoide01@kanagawa-u.ac.jp (Y.K.)

ORCID

Sotaro Kusumoto: 0000-0002-7501-383X

Manabu Nakaya: 0000-0001-8483-8131

Pierre Thuéry: 0000-0003-1683-570X

Shunsuke Nozawa: 0000-0003-4977-6849

Yang Kim: 0000-0001-8187-0793

Shinya Hayami: 0000-0001-8392-2382

Author contributions

S. Kusumoto and Y. Koide initiated and supervised the project. K. Inaba and H. Suda performed the experiments and analyzed the data. M. Nakaya and P. Thuéry carried out single crystal X-ray analysis. R. Haruki, T. Kanagawa and S. Nozawa carried out XAFS measurements. R. Tokunaga and S. Hayami carried out magnetic measurements. S. Kusumoto and Y. Kim wrote the manuscript, which was contributed by all authors. All authors have read and approved the final version of the manuscript.

Notes

The authors declare no competing financial interest.

REFERENCES

1. (a) Li, H.-Y.; Zhao, S.-N.; Zang, S.-Q.; Li, J. Functional metal–organic frameworks as effective sensors of gases and volatile compounds, *Chem. Soc. Rev.* **2020**, *49*, 6364-6401. (b) Ohkoshi, S.-i.; Tsunobuchi, Y.; Takahashi, H.; Hozumi, T.; Shiro, M.; Hashimoto, K. Synthesis and Alcohol Vapor Sensitivity of a Ferromagnetic Copper−Tungsten Bimetallic Assembly, *J. Am. Chem. Soc.* **2007**, *129*, 3084-3085. (c) Motokawa, N.; Matsunaga, S.;

Takaishi, S.; Miyasaka, H.; Yamashita, M.; Dunbar, K. R. Reversible Magnetism between an Antiferromagnet and a Ferromagnet Related to Solvation/Desolvation in a Robust Layered $[Ru_2]_2$ TCNQ Charge-Transfer System, *J. Am. Chem. Soc.* **2010**, *132*, 11943-11951. (d) Kurmoo, M. Magnetic metal–organic frameworks, *Chem. Soc. Rev.* **2009**, *38*, 1353-1379. (e) Li, H.-Y.; Zhao, S.-N.; Zang, S.-Q.; Li, J. Functional metal–organic frameworks as effective sensors of gases and volatile compounds, *Chem. Soc. Rev.* **2020**, *49*, 6364-6401.

2. (a) Miller R. G.;, Brooker, S. Reversible quantitative guest sensing via spin crossover of an iron(ii) triazole, *Chem. Sci.* **2016**, *7*, 2501-2505. (b) Hayami, S.; Komatsu Y.; Shimizu, T.; Kamihata, H.; Lee, Y. H. Spin-crossover in cobalt(II) compounds containing terpyridine and its derivatives, *Coord. Chem. Rev.*, **2011**, *255*, 1981-1990. (c) Nakaya, M.; Kosaka, W.; Miyasaka, H.; Komatsumaru, Y.; Kawaguchi, S.; Sugimoto, K.; Zhang, Y.; Nakamura, M.; Lindoy, L. F.; Hayami, S. CO_2-Induced Spin-State Switching at Room Temperature in a Monomeric Cobalt(II) Complex with the Porous Nature, *Angew. Chem. Int. Ed.* **2020**, *59*, 10658-10665. (d) Resines-Urien, E.; Piñeiro-López, L.; Fernandez-Bartolome, E.; Gamonal, A.; Garcia-Hernandez, M.; Costa, J. S. Covalent post-synthetic modification of switchable iron-based coordination polymers by volatile organic compounds: a versatile strategy for selective sensor development, *Dalton Trans.*, **2020**, *49*, 7315-7318. (e) Hayami, S.; Hashiguchi, K.; Juhasz, G.; Ohba, M.; Okawa, H.; Maeda, Y.; Kato, K.; Osaka, K.; Takata, M.; Inoue, K. 1-D Cobalt(II) Spin Transition Compound with Strong Interchain Interaction: $[Co(pyterpy)Cl_2]\cdot X$, *Inorg. Chem.* **2004**, *43*, 4124-4126. (f) Ohba, M.; Yoneda, K.; Agustí, G.; Muñoz, M. C.; Gaspar, Ana B.; Real, J. A.; Yamasaki, M.; Ando, H.; Nakao, Y.; Sakaki, S.; Kitagawa, S. Bidirectional Chemo-Switching of Spin

State in a Microporous Framework, *Angew. Chem. Int. Ed.* **2009**, *48*, 4767-4771. (g) Ohtani, R.; Hayami, S. Guest-Dependent Spin-Transition Behavior of Porous Coordination Polymers, *Chem. Eur. J.* **2017**, *23*, 2236-2248.

3. (a) Benaicha, B.; Do, K. V.; Yangui, A.; Pittala, N.; Lusson, A.; Sy, M.; Bouchez, G.; Fourati, H.; Gómez-García, C. J.; Triki, S.; Boukheddaden, K. Interplay between spin-crossover and luminescence in a multifunctional single crystal iron(ii) complex: towards a new generation of molecular sensors, *Chem. Sci.* **2019**, *10*, 6791-6798. (b) Lapresta-Fernández, A.; Titos-Padilla, S.; Herrera, J. M.; Salinas-Castillo, A.; Colacio, E.; Vallvey, L. F. C. Photographing the synergy between magnetic and colour properties in spin crossover material $[Fe(NH_2trz)_3](BF_4)_2$: a temperature sensor perspective, *Chem. Commun.* **2013**, *49*, 288-290. (c) Lapresta-Fernández, A.; Cúellar, M. P.; Herrera, J. M.; Salinas-Castillo, A.; Pegalajar, M. d. C.; Titos-Padilla, S.; Colacio, E.; Capitán-Vallvey, L. F. Particle tuning and modulation of the magnetic/colour synergy in Fe(II) spin crossover-polymer nanocomposites in a thermochromic sensor array, *J. Mater. Chem. C* **2014**, *2*, 7292-7303; (d) Sánchez-Molina, I.; Moneo-Corcuera, A.; Nieto-Castro, D.; Benet-Buchholz, J.; Galán-Mascarós, J. R. Solvent Effect on the Spin State of an Iron(II)-Triazole Trimer, *Eur. J. Inorg. Chem.* **2021**, 112–116.

4. (a) Thies, S.; Sell, H.; Schütt, C.; Bornholdt, C.; Näther, C.; Tuczek, F.; Herges, R. Light-Induced Spin Change by Photodissociable External Ligands: A New Principle for Magnetic Switching of Molecules, *J. Am. Chem. Soc.* **2011**, *133*, 16243-16250. (b) Venkataramani, S.; Jana, U.; Dommaschk, M.; Sönnichsen, F. D.; Tuczek, F.; Herges, R. Magnetic bistability of molecules in homogeneous solution at room temperature, *Science* **2011**, *331*, 445; (c) Dommaschk, M.; Gutzeit, F.; Boretius, S.; Haag, R.; Herges, R. Coordination-

Induced Spin-State-Switch (CISSS) in water, *Chem. Commun.* **2014**, *50*, 12476-12478. (d) Nowak, R.; Prasetyanto, E. A.; Cola, L. D.; Bojer, B.; Siegel, R.; Senker, J.; Rösslerd, E.; Weber, B. Proton-driven coordination-induced spin state switch (PD-CISSS) of iron(ii) complexes, *Chem. Commun.* **2017**, *53*, 971-974; (e) Kurz, H.; Schötz, K.; Papadopoulos, I.; Heinemann, F. W.; Maid, H.; Guldi, D. M.; Köhler, A.; Hörner, G.; Weber, B. A Fluorescence-Detected Coordination-Induced Spin State Switch, *J. Am. Chem. Soc.* **2021**, *143*, 3466−3480; (f) Klaß, M.; Krahmer, J.; Näther, C.; Tuczek, F.; Design, synthesis, and evaluation of nickel dipyridylmethane complexes for Coordination-Induced Spin State Switching (CISSS), *Dalton Trans.* **2018**, *47*, 1261-1275. (g) Reczynski, M.; Chorazy, S.; Nowicka, B.; Sieklucka, B.; Ohkoshi, S.-i. Dehydration of Octacyanido-Bridged Ni^{II}-W^{IV} Framework toward Negative Thermal Expansion and Magneto-Colorimetric Switching, *Inorg. Chem.* **2017**, *56*, 179-185. (h) Funasako, Y.; Mochida, T.; Takahashi, K.; Sakurai, T.; Ohta, H. Vapochromic Ionic Liquids from Metal–Chelate Complexes Exhibiting Reversible Changes in Color, Thermal, and Magnetic Properties, *Chem. Eur. J.* **2012**, *18*, 11929-11936.

5. (a) Kar, P.; Yoshida, M.; Shigeta, Y.; Usui, A.; Kobayashi, A.; Minamidate, T.; Matsunaga, N.; Kato, M. Methanol-Triggered Vapochromism Coupled with Solid-State Spin Switching in a Nickel(II)-Quinonoid Complex, *Angew. Chem. Int. Ed.* **2017**, *56*, 2345-2349; (b) Fgrpaß, K. M.; Peschel, L. M.; Schachner, J. A.; Borisov, S. M.; Krenn, H.; Belaj, F.; Mösch-Zanetti, N. C. Vapochromism and Magnetochemical Switching of a Nickel(II) Paddlewheel Complex by Reversible NH_3 Uptake and Release, *Angew. Chem. Int. Ed.* **2021**, *60*, 13401-13404. (c) Zhao, Y.; Wang, L.; Xue, S.; Guo, Y. Reversible coordination-induced spin state switching in a nickel(ii) complex via a crystal-to-crystal transformation,

Inorg. Chem. Front. **2022**, *9*, 4127-4135; (d) Xue, S.; Solre, G. F. B.; Wang, X.; Wang, L.; Guo, Y. Vapor-triggered reversible crystal transformation of a nickel-based magnetic molecular switch, *Chem. Commun.* **2022**, *58*, 1954-1957.

6. Xuea M.-X.; and Liu, S.-X. Bis[2-hydroxy-*N*'-(3-phenylprop-2-enylidene)benzohydrazidato-κ^2N',O]-bis(methanol-κO)nickel(II) and bis[2-hydroxy-N'-(3-phenylprop-2- enylidene)benzohydrazidato-κ^2N',O]- bis(pyridine-κN)nickel(II), *Acta Cryst.* **2008**, C64, m190–m193.
7. Kusumoto, S.; Sugimoto, A.; Zhang, Y.; Kim, Y.; Nakamura, M.; Hayami, S. Elastic Crystalline Fibers Composed of a Nickel(II) Complex, *Inorg. Chem.* **2021**, *60*, 1294-1298.
8. (a) Kusumoto, S.; Kim, Y.; Nakamura, M.; Lindoy, L. F.; Hayami, S. Ferromagnetically Coupled Hydroxo-bridged Heptanuclear Ni(II) Wheel Cluster with S = 7 Ground Spin State, *Chem. Lett.* **2020**, *49*, 24-27; (b) Kusumoto, S.; Kobayashi, F.; Ohtani, R.; Zhang, Y.; Harrowfield, J.; Kim, Y.; Hayami, S.; Nakamura, M. Creating capsules with cubanes, *Dalton Trans.* **2018**, *47*, 9575-9578.
9. (a) Mackenzie, C. F.; Spackman, P. R.; Jayatilaka, D.; Spackman, M. A. CrystalExplorer model energies and energy frameworks: extension to metal coordination compounds, organic salts, solvates and open-shell systems, *IUCrJ*, **2017**, *4*, 575; (b) Turner, M. J.; McKinnon, J. J.; Wolff, S. K.; Grimwood, D. J.; Spackman, P. R.; Jayatilaka, D.; Spackman, M. A. CrystalExplorer17, 2017. University of Western Australia, https://hirshfeldsurface.net.
10. (a) Yano, R.; Yoshida, M.; Tsunenari, T.; Sato-Tomita, A.; Nozawa, S.; Iida, Y.; Matsunaga, N.; Kobayashi, A.; Kato, M. Vapochromic behaviour of a nickel(II)-quinonoid complex with dimensional changes between 1D and higher, *Dalton Trans.* **2021**, *50*, 8696-

8703; (b) Escuer, A.; Castro, I.; Mautner, F.; Fallah, M. S. E.; Vicente, R. Magnetic Studies on μ-Azido Polynuclear Nickel(II) Compounds with the 222-tet Ligand. Crystal Structure of $(\mu\text{-}N_3)_2[Ni(222\text{-tet})]_2(BPh_4)_2$ (222-tet = Triethylenetetramine) and EXAFS Structural Characterization of the Triangular Compounds $(\mu\text{-}N_3)_3[Ni(222\text{-tet})]_3(X)_3$ ($X = PF_6^-$, ClO_4^-), *Inorg. Chem.* **1997**, *36*, 4633-4640.

For Table of Contents Use Only

Coordination-induced spin-state switching (CISSS) and color change of new labile Ni(II) complexes by pyridine vapor in a short time result in a geometric transformation between four- and six-coordinate based on pyridine coordination/decoordination.